EFFICIENT OPERATION OF HYBRID PHOTOVOLTAIC-THERMOELECTRIC SYSTEM COMBINED WITH MICRO-CHANNEL HEAT SINK

Ahmed Abdo[1], Mahmoud Ahmed[1], Hamdy hassan[1], and Shinichi Ookawara[1, 2]
[1] Department of Energy Resources Engineering, Egypt-Japan University of Science and Technology (E-JUST), Alexandria, Egypt
[2] Tokyo Institute of Technology, Tokyo, Japan
Corresponding author: Ahmed Abdo, e-mail: Ahmed.abdo@ejust.edu.eg

REFERENCE NO

PELT-01

Keywords:
Thermoelectric, Photovoltaic, Micro-channel Heat Sink, and Heat Transfer.

ABSTRACT

Concentration of solar irradiance on photovoltaic cells causes a significant increase in cell temperature which considerably decreases its electrical conversion efficiency. In contrast, high temperature difference is essential to generate a large amount of power from thermoelectric modules. So, using hybrid solar concentration photovoltaic-thermoelectric system combined with micro-channels is a desperate need that will increase the system overall efficiency. Therefore, in this study, a three-dimensional comprehensive model is developed. The model is numerically simulated by ANSYS Workbench v. 17.2. with important variables such as input solar energy and micro-channel coolant flow rate were included to control photovoltaic cell temperature lower than critical point (i.e. 85 ℃)and enhance temperature difference between the thermoelectric surfaces (i.e. hot &cold) higher than 150 ℃. The system is operated with different values of solar concentration ratios and coolant mass flow-rate. The results shown that using thermoelectric generator in parallel with photovoltaic will enhance the overall system efficiency to certain values. More so, the proposed system attains its maximum solar irradiance efficient for safe operation of the systems component.

1. INTRODUCTION

To make environment, surrounding clean and free of pollution, we should reduce carbon emissions from conventional power stations, or search for friendly power station like solar systems[1]. Solar system could be of high capacity like central receiver system or medium or low capacity like photovoltaic (PV). Solar PV systems are considered as always a good choice for medium and low capacity. Solar Thermoelectric Generator (STEG) also could be used for generation of electricity. As absorber plate with high absorptivity surface is used in harvesting majority of incident solar energy[2, 3].Both PV and STEG are use as direct conversion devices that could be affected by operating temperature. As known increasing of PV cell temperature decreases the conversion efficiency and may cause material failure [4]. Another view with Thermoelectric Generator (TEG), is the increase of hot side surface temperature at certain level and at constant value of the cold side surface temperature which enhances the conversion efficiency[1] . Obviously, using solar concentrator (SC) to get more absorbed solar energy, means more generated electricity, in addition to higher body temperature which is good for TEG and not good for PV, as earlier highlighted. Definitely, SC is a powerful tool for increasing absorbing energy by PV, or STEG systems. Cooling heat sink (HS) is also very important in treating SC side effects on PV material (i.e. control its temperature below critical point 85℃). Also HS helps to increase temperature difference between its surfaces by increasing its convention efficiency [5] and if it is required, the remaining thermal energy absorbed by cooling fluid could be used for heating applications. Cooling can be natural or forced convection while, air, water, or Phase Change Material (PCM) material could be used as working material [6]. Merging between PV and TEG in one system is acceptable concept to achieve better utility of input solar energy [7]. Many scientific researchers are interested in some of those systems. Ravita Lamba et al., [8] presented a theoretical thermodynamic model to analyse

the performance of a concentrated PV–TEG hybrid system that was solved and optimized using MATLAB. Guiqiang Li. et al, [9] studied on contact methods between PV and TEG (new system consisting of PV, and TEG). M. Hajji et al, [10] reported on Saturated Water flowing through flat micro-channel, transporting heat from PV (i.e. evaporator) to hot surface of TEG (i.e. condenser) with the cold surface of TEG is cooled by fins.

In another hand there are some researchers worked on performance of indirect contact between PV and TEG. They studied a new concept based on an indirect (i.e. instead of direct) photovoltaic and thermoelectric coupling with a concentrator is placed between PV and TEG without any physical contact of the three components. They used different values solar concentration up to 2000 Watt per meter square with variable cooling capacity. The results revealed that an indirect coupling is an interesting choice to maximize solar energy investment that will give maximum overall efficiencies of 20%, and 28% for uncooled and cooled systems, respectively. Willars-Rodríguez, et al., [11] studied experimentally a PV-TEG hybrid system where both the PV and TEG absorb solar energy with PV material was silicon, while TEG material was bismuth-Telluride. The Fresnel lens was used for TEG, whereas PV module was non-concentrated. The results revealed that a thermal hybrid solar system of a PV-TEG-radiation concentrator was able to provide high electrical and thermal efficiency with relatively low cost. PV-TEG hybrid systems PV-TEG hybrid systems could be classified into many types [12]. In majority configurations of PV-TEG hybrid systems, the TEG gets its input heat from PV back surface. So, the critical issue here is the operating temperature of contact surface between PV and TEG. Increasing the operating temperature of PV-TEG contact surface will improve the performance of TEG and decreases the performance of PV and may be causes damage for its material [11].

In the present numerical study we proposed a new configuration hybrid PV-STEG with common HS for both, absorbs excess heat from PV cell to adjust it temperature to acceptable value, and at the same time, increase the temperature difference between TEG surfaces. In this configuration decreasing cell temperature will help improve both PV and STEG performance and expect that the configuration will solve some weak points in other used configurations.

This study aimed at investigating and analysing new configuration of hybrid none concentrated PV-concentrated -STEG that is cooled by wide micro-channel heat sink and also to study the effect of water flow rate on the system performance at different values of solar concentration for STEG.

.

2. General view of proposed physical model

The current study includes a new designed configuration of solar PV-STEG hybrid system as shown in Fig. 1. The main components of system studied are solar concentrator (Parabolic trough), PV solar cell, STEG, and micro-channel HS. The STEG is consist of solar absorber plate and TEG [3]. The Geometry of solar absorber is $L_{ab}, W_{ab}, \delta_{ab}$ with PV solar cell that has number of layers, Glass, and silicon layers. The silicon layer is put inside transparent ethylene vinyl acetate (EVA) layer to save it and the final layer is the tedlar polymer layer, a photo-stable layer made of polyvinyl fluoride (PVF). [13] and the used HS is wide micro channel made from aluminium [14] with water flowing through $H_{water} = 0.1\ mm$ micro-channel with hydraulic diameter of $D_{water} = 0.2mm$. The detailed geometry is presented in table 1 and important properties material used as shown in table 2. In the current work, wide HS is sandwiched between PV solar cell and STEG.

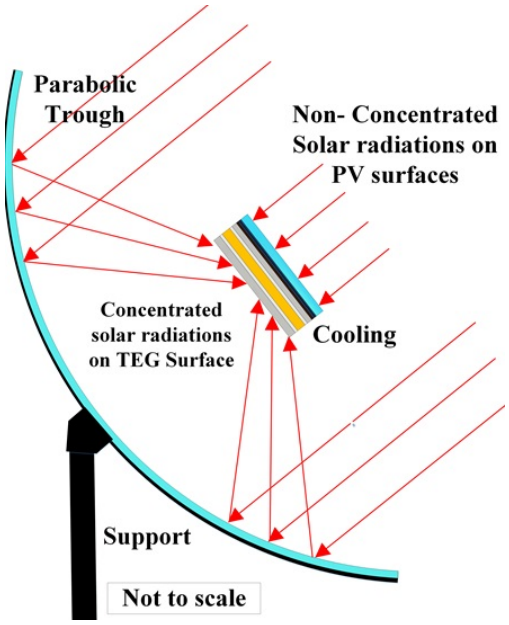

Fig. 1. Physical Description.

Table 1. Geometry of PV-STEG

Part Name	Dimension
Glass layer	125mmx31.25mmx3mm
Up EVA layer	125mmx31.25mmx0.5mm
SI Layer	125 x31.25mmx0.2mm
lower EVA layer	125mmx31.25mmx0.5mm
Tedlar	125mmx31.25mmx0.3mm
Channel thickness	0.1mm
Ceramic layer (hot-cold)	125mmx31.25mmx0.8mm
Electrical connections	1.5mmx1.5mmx0.15mm
Legs of TEG	1.5mmx1.5mmx5mm

Table 2. Surface Optical Properties

property	**(ρ)**	**(τ)**	**(α)**	**(ε)**
Glass	0.04	0.95	0.04	0.85
silicon	0.08	0.02	0.9	-
EVA	0.02	0.9	0.08	0.9
TED	0.86	0.012	0.128	0.9
TEG Absorber	-	-	0.9	0.15

3. EQUATIONS

3.1. PV module

General heat transfer through layers including PV layers TEG Layers and channel walls by conduction in Cartesian coordinates[15, 16] is as follows;

$$\rho . C_p . \frac{\partial T}{\partial t} = \nabla . (q) + Q \qquad (1)$$

Where ρ is the solid density, C_p is solid specific heat at constant pressure, q is heat transfer by conduction, and Q heat generation per unit volume

For study state conditions $\frac{\partial T}{\partial t} = 0$

$$0 = \nabla . (q) + Q \qquad (2)$$

$$q = \kappa_{layer} \nabla T \qquad (3)$$

Where κ_{layer} is thermal conductivity of layer

The equations related to power generation and conversion efficiency of PV[17]

$$E_{elec,pv} = \eta_{Sc} . \tau_g . \tau_{t,EVA} . (G) \qquad (4)$$

$$\eta_{Sc} = \eta_{ref} (1 - \beta_{ref} . (T_{sc} - T_{ref})) \qquad (5)$$

Where: $\boldsymbol{\eta_{ref}}$ and $\boldsymbol{\beta_{ref}}$ are the solar cell efficiency and temperature coefficient at a reference temperature of $\boldsymbol{T_{ref} = 25}$℃ respectively. Symbol $(\boldsymbol{G})$ is for the net concentrated solar radiation incident on the solar system surfaces regardless of the concentrator's optical losses.

The rates of heat transfer though interface between solar cell layers could be calculated as following.

$$q_1 = q_2 = \kappa_1 \nabla T = \kappa_2 \nabla T \qquad (6)$$

Where: subtitle 1, 2 related to layer that heat transfer from, layer heat transfer to it respectively.

3.2. STEG module

STEG consisted from Absorber and TEG[18]. Solar energy absorbed by absorber is calculated from the next equation.

$$Q_{abs} = \alpha_{abs} . G \qquad (7)$$

Where: symbol α_{abs} is the absorptivity of used absorber.

The properties of studied TEG are depending on its material temperature, so its general governing equation could be rearranged as following[19]

$$0 = \nabla.(\kappa\nabla T) + \frac{J^2}{\sigma} - TJ.\nabla\alpha \quad (8)$$

Where $\frac{J^2}{\sigma}$, J , $TJ.\nabla\alpha, (\kappa\nabla T)$ are joule heat , heat transfer by conduction , generated power due to conversion of heat in to electrical energy through seebeck respectively.

3.3. Wide micro-channel.

General Governing equations that control the flow of water through micro-channel are numerically solved by finite volume (fluent) [20]

Mass conservation

$$\nabla.\left(\rho\vec{V}\right) = 0 \quad (9)$$

Momentum conservation

$$\vec{V}.\nabla\left(\rho\vec{V}\right) = \nabla P + \nabla.(\mu\nabla.\vec{V}) \quad (10)$$

Energy conversation

$$\vec{V}.\nabla(\rho.C_f.T_f) = \nabla.(\kappa\nabla T_f) \quad (11)$$

4. NUMERICAL SOLUTION

A numerical model using ANSYS Workbench v. 17.2 for numerical computation, based on multi-physics equations such as heat transfer, fluid mechanics and thermoelectricity was developed to predict both thermal and electrical powers of PV and TEG.

4.1. Mesh independent test

A mesh independence test is performed to reach accurate results independent of the number of grids. It is found that the solar cell temperature changes slowly with the further increase of the number of grid cells greater than 16,708,450 for the whole domain. The simulations were performed using Dell Precision T7500 workstation With Intel Xeon® processor of 3 GH, 40-Processors.

4.2. MODEL VALIDATION.

The studied Model includes three parts, PV, STEG, and Micro-channel. Each part was validated as following.

4.2.1. Solar Cell Model Validation

Fig. 2, is the model of studied PV cell validated with experimental results[21]. The results are in good range.

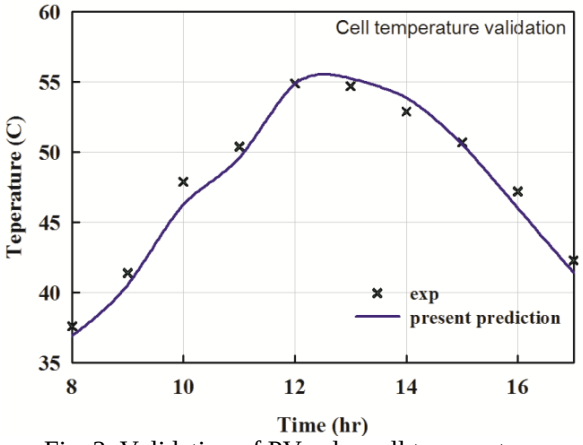

Fig. 2. Validation of PV solar cell temperature

4.2.2. STEG Model Validation

STEG model was validated with theoretical results [22] the results shown a maximum deviation of 2% in efficiency. The method to simulate thermoelectric generator was taken from[23].

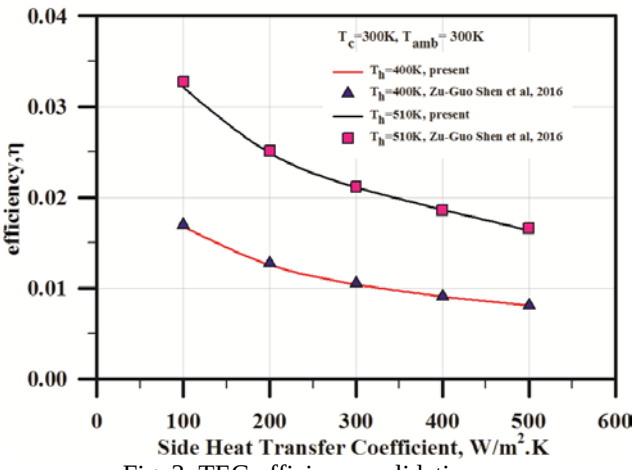

Fig. 3. TEG efficiency validation.

4.2.3. Micro-channel Model Validation

According to the description and dimension of micro channel, it is look like channel between two extended plates and could be solved as two dimensions. Velocity profile was compared with theoretical velocity profile predicted from the next exact equation. As reported [24, 25]

$$u = (3u_m/2) * (1 - \left(\frac{y}{b}\right)^2) \quad (12)$$

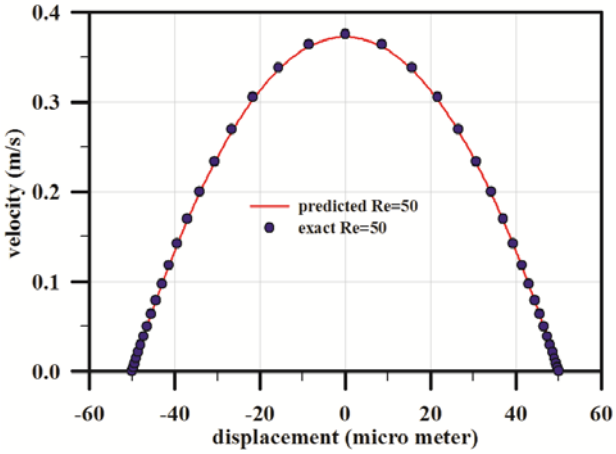

Fig. 4. Velocity profile for laminar fully developed flow at Reynolds number =50

5. RESULTS AND DISCUSSIONS.

The results are presented in three subsections. The first subsection demonstrates the variation of average temperature for PV cell, and TEG surfaces (i.e. hot and cold) with water flow rate, and the effect of concentration ratio on STEG. The second subsection presents the effect of cooling water mass flow rate on PV-STEG efficiencies under different values of concentration ratio. While the third subsection report on how to select operating point for studied system.

5.1. Surfaces Temperature

Surfaces temperatures jump with solar concentration increase and gradually decrease with more water flow rate until certain value according to their thermal properties of studied material (i.e. value of thermal conductivity). Fig 5-a shown the average temperature of PV solar cell have reached to about $305K$ for all values of solar concentration incident on STEG surface and at Re=100. The results reveal that the effect of TEG on PV temperature is small at high concentration ratio and that is a good point in new configuration. Figs. 5-b, 5-c shown the effect of solar concentration on temperature difference between hot and cold side of TEG is higher than cooling effect as the temperature difference changes from about 23K to 140K when concentration ratio on STEG changes from 3 suns to 20 suns, respectively.

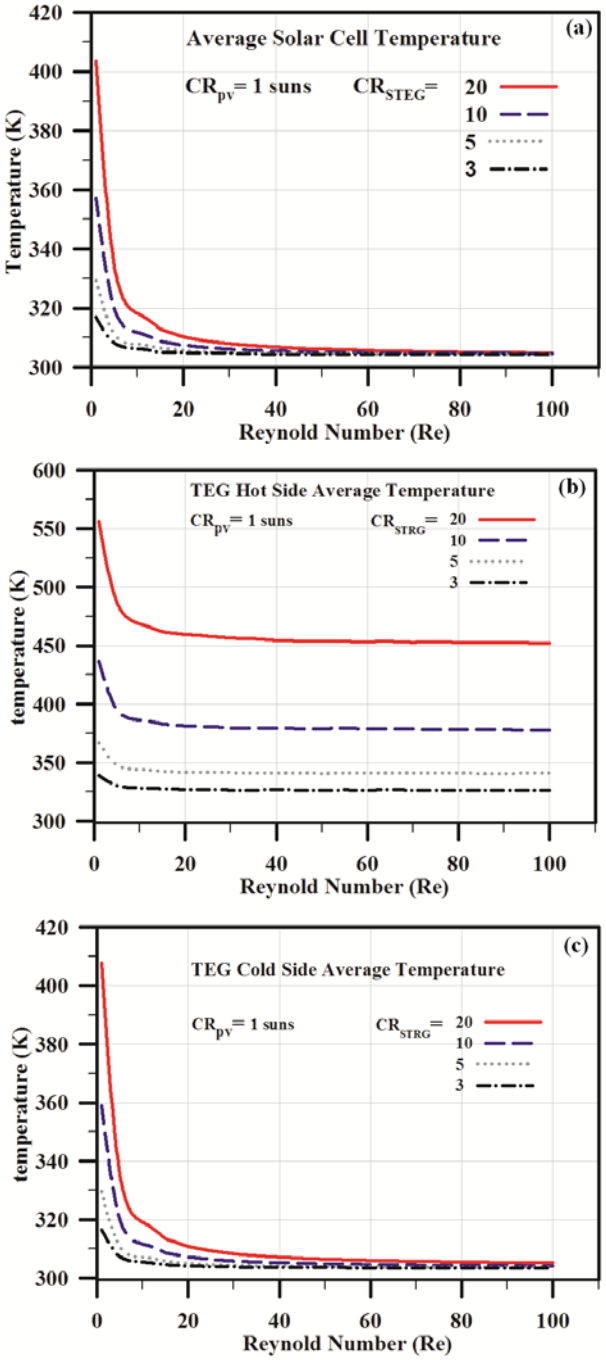

Fig. 5. (a) Average temperature of PV solar cell, (b)

Average temperature of TEG hot side, and (c) Average temperature of TEG cold side

5.2. PV-STEG efficiencies

As seen in Fig.6-a and as discussed in previous subsection the temperature of PV solar cell is slightly affected by changing solar concentration incident on STEG. So at high water flow rate the PV conversion efficiency has constant value which is about 0.194 at Re = 100. More over the conversion efficiency of STEG becomes better at high concentrations ratio as shown in Fig.6-b with maximum and minimum STEG efficiency is about 0.006441 and 0.036291.

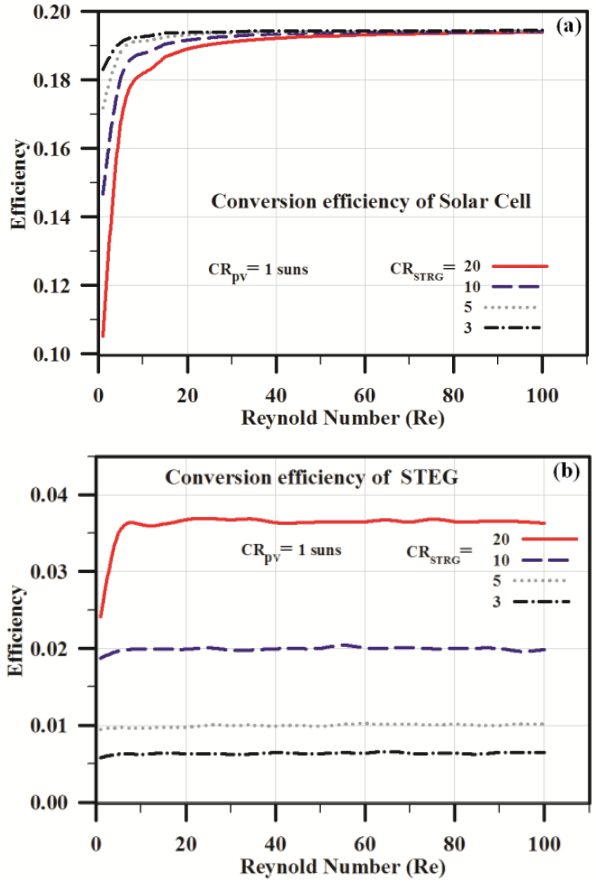

Fig. 6. (a) PV solar cell conversion efficiency ,and (b) STEG conversion efficiency

5.3. Net Power generated

As shown in Figures 7-a, and 7-b the operating points for investigated system can be developed from separation point between total power generated curve, and net power curve. For CR_{STEG}= 20, and 3 suns, the operating point are at Re= 40, and 20 respectively. Due to increasing Reynolds number (i.e. increasing flow velocity), the power consumed against friction between water flow and channel wall increases.

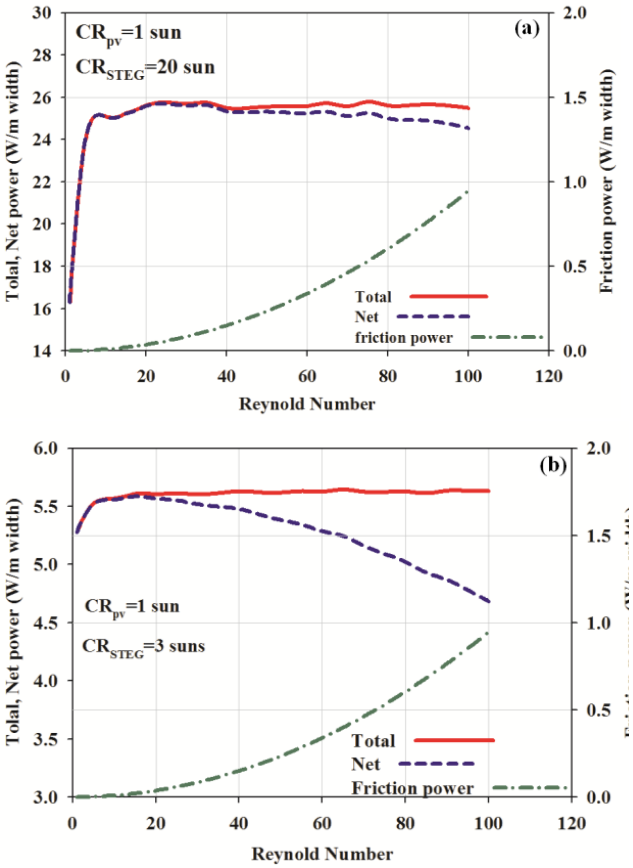

Fig. 7. (a) Whole system operating point at 20 suns for STEG
and (b) Whole system operating point at 3 suns for STEG

3. CONCLUSIONS

From results and discussion we could conclude that the proposed Parallel PV-STEG configuration has ability to generate more power at good conversion efficiency for both PV and STEG when the efficiency of PV solar cell remain constant with high value at different values of solar concentration incident on STEG. Moreover efficiency of STEG is enhanced with higher value of concentration ratio incident on STEG absorber with slight effect on PV solar cell temperature especially at high water flow rate (i.e. higher Re).

Acknowledgements
Authors wish to thanks Egypt-Japan University of Science and Technology for its supports.

Nomenclature

C	Specific heat of coolant
H	height
D	Hydraulic Diameter
W	width
k	Thermal conductivity
L	length
m	Mass flow rate
E	power
Re	Reynolds number
T	temperature
u	Velocity component in x direction

Greek Letters

α	Absorptivity , seebeck coefficient
τ	transmissivity
ε	emissivity
μ	Fluid dynamic viscosity
σ	Stephan-Boltzmann constant
β	Solar cell temperature coefficient
δ	thickness
λ	Molecular mean free path
η	Electrical efficiency – thermal efficiency

Subtitles

a	ambient
leg	Thermoelectric legs
ab	absorber coated aluminium substrate

References

[1] P. Li, L. Cai, P. Zhai, X. Tang, Q. Zhang, M. Niino, Design of a concentration solar thermoelectric generator, Journal of electronic materials, 39 (2010) 1522-1530.
[2] L. Liu, X.S. Lu, M.L. Shi, Y.K. Ma, J.Y. Shi, Modeling of flat-plate solar thermoelectric generators for space applications, Solar Energy, 132 (2016) 386-394.
[3] K. Sudharshan, V.P. Kumar, H.C. Barshilia, Performance evaluation of a thermally concentrated solar thermo-electric generator without optical concentration, Solar Energy Materials and Solar Cells, 157 (2016) 93-100.
[4] A. Radwan, M. Ahmed, S. Ookawara, Performance enhancement of concentrated photovoltaic systems using a microchannel heat sink with nanofluids, Energy Conversion and Management, 119 (2016) 289-303.
[5] P. Sundarraj, D. Maity, S.S. Roy, R.A. Taylor, Recent advances in thermoelectric materials and solar thermoelectric generators–a critical review, RSC Advances, 4 (2014) 46860-46874.
[6] T. Cui, Y. Xuan, E. Yin, Q. Li, D. Li, Experimental investigation on potential of a concentrated photovoltaic-thermoelectric system with phase change materials, Energy, 122 (2017) 94-102.
[7] T. Cui, Y. Xuan, Q. Li, Design of a novel concentrating photovoltaic–thermoelectric system incorporated with phase change materials, Energy Conversion and Management, 112 (2016) 49-60.
[8] R. Lamba, S. Kaushik, Modeling and performance analysis of a concentrated photovoltaic–thermoelectric hybrid power generation system, Energy Conversion and Management, 115 (2016) 288-298.
[9] G. Li, X. Zhao, J. Ji, Conceptual development of a novel photovoltaic-thermoelectric system and preliminary economic analysis, Energy Conversion and Management, 126 (2016) 935-943.
[10] M. Hajji, H. Labrim, M. Benaissa, A. Laazizi, H. Ez-Zahraouy, E. Ntsoenzok, J. Meot, A. Benyoussef, Photovoltaic and thermoelectric indirect coupling for maximum solar energy exploitation, Energy Conversion and Management, 136 (2017) 184-191.
[11] F. Willars -Rodrígue
P. Vorobiev, Y.V. Vorobiev, Investigation of solar hybrid system with concentrating Fresnel lens, photovoltaic and thermoelectric generators, International Journal of Energy Research, 41 (2017) 377-388.
[12] C. Babu, P. Ponnambalam, The role of thermoelectric generators in the hybrid PV/T systems: A review, Energy Conversion and Management, 151 (2017) 368-385.
[13] S. Armstrong, W. Hurley, A thermal model for photovoltaic panels under varying atmospheric conditions, Applied Thermal Engineering, 30 (2010) 1488-1495.
[14] L. Micheli, E.F. Fernández, F. Almonacid, T.K. Mallick, G.P. Smestad, Performance, limits

and economic perspectives for passive cooling of High Concentrator Photovoltaics, Solar Energy Materials and Solar Cells, 153 (2016) 164-178.
[15] A. Radwan, M. Ahmed, The influence of microchannel heat sink configurations on the performance of low concentrator photovoltaic systems, Applied Energy, 206 (2017) 594-611.
[16] M. Siddiqui, A. Arif, Electrical, thermal and structural performance of a cooled PV module: Transient analysis using a multiphysics model, Applied energy, 112 (2013) 300-312.
[17] M. Hedayatizadeh, Y. Ajabshirchi, F. Sarhaddi, A. Safavinejad, S. Farahat, H. Chaji, Thermal and electrical assessment of an integrated solar photovoltaic thermal (PV/T) water collector equipped with a compound parabolic concentrator (CPC), International journal of green energy, 10 (2013) 494-522.
[18] A.A. Candadai, V.P. Kumar, H.C. Barshilia, Performance evaluation of a natural convective-cooled concentration solar thermoelectric generator coupled with a spectrally selective high temperature absorber coating, Solar Energy Materials and Solar Cells, 145 (2016) 333-341.
[19] H. Lee, Thermoelectrics: Design and Materials, John Wiley & Sons2016.
[20] A. Radwan, S. Ookawara, M. Ahmed, Analysis and simulation of concentrating photovoltaic systems with a microchannel heat sink, Solar Energy, 136 (2016) 35-48.
[21] A. Joshi, A. Tiwari, G. Tiwari, I. Dincer, B. Reddy, Performance evaluation of a hybrid photovoltaic thermal (PV/T)(glass-to-glass) system, International Journal of Thermal Sciences, 48 (2009) 154-164.
[22] Z.-G. Shen, S.-Y. Wu, L. Xiao, G. Yin, Theoretical modeling of thermoelectric generator with particular emphasis on the effect of side surface heat transfer, Energy, 95 (2016) 367-379.
[23] F. Brito, L. Figueiredo, L. Rocha, A. Cruz, L. Goncalves, J. Martins, M. Hall, Analysis of the Effect of Module Thickness Reduction on Thermoelectric Generator Output, Journal of Electronic Materials, 45 (2016) 1711-1729.
[24] M. Ebadian, Z. Dong, Forced convection, internal flow in ducts, McGraw Hill, New York, 1998.
[25] S. Kandlikar, S. Garimella, D. Li, S. Colin, M.R. King, Heat transfer and fluid flow in minichannels and microchannels, elsevier2005.